



1 Stream water sourcing from high elevation snowpack inferred from 2 stable isotopes of water: A novel application of *d-excess* values

3 Matthias Sprenger^{1*}, Rosemary W.H. Carroll², David Marchetti³, Carleton Bern⁴, Harsh Beria⁵, Wendy Brown⁶,
4 Alexander Newman⁶, Curtis Beutler⁶, Kenneth H. Williams^{1,6}

5 ¹Lawrence Berkeley National Laboratory, Berkeley, CA, USA

6 ²Desert Research Institute, Reno, NV, USA

7 ³Western Colorado University, Gunnison, CO, USA

8 ⁴U.S. Geological Survey, Denver, CO, USA

9 ⁵Department of Environmental Systems Science, ETH Zurich, Zurich, Switzerland

10 ⁶Rocky Mountain Biological Laboratory, Crested Butte, CO, USA

11 *Corresponding author: msprenger@lbl.gov

12

13 **Abstract.** About 80% of the precipitation in the Colorado River's headwaters is snow, and the resulting snowmelt-
14 driven hydrograph is a crucial water source for about 40 million people. Snowmelt from alpine and subalpine
15 snowpack contributes substantially to groundwater recharge and river flow. However, the dynamics of snowmelt
16 progression are not well understood because observations of the high elevation snowpack are difficult due to
17 challenging access in complex mountainous terrain as well as the cost- and labor-intensity of methods. We present a
18 novel approach to infer the processes and dynamics of high elevation snowmelt contributions predicated upon stable
19 hydrogen and oxygen isotope ratios observed in stream discharge. We show that *d-excess* values of stream water can
20 serve as a comparatively cost-effective proxy for a catchment integrated signal of high elevation snow melt
21 contributions to catchment runoff.

22 We sampled stable hydrogen and oxygen isotope ratios of the precipitation, snowpack, and stream water in the East
23 River, a headwater catchment of the Colorado River and the stream water of larger catchments at sites on the Gunnison
24 River and Colorado River.

25 The *d-excess* of snowpack increased with elevation; the upper subalpine and alpine snowpack (>3200 m) and had a
26 substantially higher *d-excess* compared to lower elevations (<3200 m) in the study area. The *d-excess* values of stream
27 water reflected this because *d-excess* values increased as the higher elevation snowpack contributed more to stream
28 water generation later in the snowmelt/runoff season. Endmember mixing analyses based on the *d-excess* data showed
29 that the share of high elevation snowmelt contributions within the snowmelt hydrograph was on average 44% and
30 generally increased during melt period progression, up to 70%. The observed pattern was consistent during six years
31 for the East River, and a similar relation was found for the larger catchments on the Gunnison and Colorado Rivers.



32 High elevation snowpack contributions were found to be higher for years with lower snowpack and warmer spring
33 temperatures. Thus, we conclude that the *d-excess* of stream water is a viable proxy to observe changes in high
34 elevation snowmelt contributions in catchments at various scales. Inter-catchment comparisons and temporal trends
35 of the *d-excess* of stream water could therefore serve as a catchment-integrated measure to monitor if mountain
36 systems increasingly rely on high elevation water inputs during snow drought.

37 1 Introduction

38 The snowpack in mountainous regions provides a crucial water source for the ecosystems and human activities
39 downstream (Immerzeel et al., 2020). In the alpine and subalpine headwaters of semi-arid regions where the summer
40 precipitation contribution to streamflow is usually relatively low, as in the southwestern United States, snowmelt
41 sustains streamflow during much of the growing season when water demands are higher. The Colorado River plays a
42 special role in the hydrology of the southwestern United States because its headwaters in the Rocky Mountains support
43 the water supply for about 40 million people, agriculture, industry and power generation (Bureau of Reclamation,
44 2012). The snowmelt from high elevation upper subalpine and alpine regions of the mountainous headwaters of the
45 Colorado River was shown to be particularly important for the groundwater recharge and sustaining river flow (Carroll
46 et al., 2019). However, observed (Faybishenko et al., 2022; Hoerling et al., 2019) and projected (Bennett and Talsma,
47 2021) increases in air temperatures in the headwaters of the Colorado River can lead to a decrease of the snow-to-rain
48 ratio during the coming decades (Hammond et al., 2023). Therefore, if carbon emissions are not reduced, the
49 mountainous catchments in the Colorado River could likely transition towards low-to-no snow conditions during the
50 second half of this century (Siirila-Woodburn et al., 2021). Because we already observe a general trend towards lower
51 snow packs and earlier snowmelt in the western United States (Musselman et al., 2021), it is crucial to better
52 understand the role of high elevation snowpack in streamflow dynamics. However, the tools needed to observe high
53 elevation snowmelt processes are either missing (e.g. point observations), too coarse a resolution (e.g. satellite), or
54 expensive to obtain (e.g. airborne lidar techniques, numerical models), which is why we investigate the use of a stable
55 isotope-based method that can help assess upper subalpine and alpine snowmelt contributions to streamflow.

56 Snowpack assessments and snowmelt dynamics are usually monitored with point observations like the U.S. Natural
57 Resource Conservation Service's (NRCS) SNOW TELemetry (SNOTEL) network (Report Generator 2.0, 2023).
58 However, the highest elevations in the western United States are not covered by this network (max. elevation 3543 m
59 a.s.l.), despite this area harboring the largest snow water equivalent (SWE) and most surface water input volumes per
60 square meter (Hammond et al., 2023). Therefore, while the measured snow pack at SNOTEL sites will indicate melt-
61 out, there remains substantial snow cover in the alpine regions past the SNOTEL indicated melt-out dates (Dozier et
62 al., 2016). To obtain a spatial representation of the SWE from the SNOTEL point measurements, regression analyses
63 with physiographic variables (e.g., elevation, slope, aspect) are commonly used (Fassnacht et al., 2003). Heterogeneity
64 of snowfall accumulation and redistribution of snow (Freudiger et al., 2017) in complex mountainous terrain makes
65 such interpolation and extrapolation efforts difficult (Dozier et al., 2016). Adding information about the previous
66 year's snow cover distribution from satellite data was shown to improve the reconstruction of SWE across the complex
67 mountainous terrain of the Upper Colorado River Basin (Schneider and Molotch, 2016). However, maps of snowpack



68 distribution from airborne snow observatory (ASO) based on airborne light-detection (Painter et al., 2016) are costly
69 and therefore may not be applicable across multiple mountainous catchments and/or during several years.

70 In addition to the high costs and labor intensity of the currently available methods to study high elevation snowmelt
71 dynamics, these approaches are generally limited to hydrometric data and do not include any tracer information. Beria
72 et al. (2018) outlined multiple ways how stable hydrogen and oxygen isotopes of water ($\delta^2\text{H}$ and $\delta^{18}\text{O}$) can provide
73 valuable insights into snow hydrological processes. Because hydrogen and oxygen isotopes comprise the water
74 molecule, $\delta^2\text{H}$ and $\delta^{18}\text{O}$ signatures are ideal tracers to track fluxes in the water cycle (Kendall and McDonnell, 1998).
75 The relationship between the relative stable hydrogen and oxygen isotope ratios of water systems was identified by
76 Craig (1961) as

$$77 \quad \delta^2\text{H} = 8 \times \delta^{18}\text{O} + 10 \quad (1)$$

78 who characterized this relationship as indicative of “waters which have not undergone excessive evapotranspiration.”
79 (Dansgaard, 1964) defined the concept of deuterium-excess, or *d-excess*, as

$$80 \quad d\text{-excess} = \delta^2\text{H} - 8 \times \delta^{18}\text{O} \quad (2)$$

81 which can be interpreted as an index of non-equilibrium in the simple condensation - evaporation of global
82 precipitation. This formulation has been useful for screening isotopic results from water samples: values of *d-excess*
83 between 10 and 11 are effectively the intercept in Craig’s proposed relationship and indicate quasi-stable conditions
84 at a relative humidity of ~85% (Dansgaard, 1964; Gat, 2000). Here, we test two hypotheses to examine how *d-excess*
85 data from stream water samples are related to high elevation snowmelt contributions to the catchment runoff during
86 the snowmelt periods. First, we hypothesize that *d-excess* values in stream water during the snowmelt hydrograph
87 reflect the changing dominance of snowmelt contributions through time from lower to higher elevations. Second, we
88 test if these patterns of *d-excess* of stream water are detectable across ranges in drainage area, thus increasing their
89 broader applicability.

90

91 **2 Methods**

92 **2.1 Study sites and data**

93 Our study is situated in the headwaters region of the Upper Colorado River (Figure 1) with a focus on an East River
94 subcatchment (85 km²) as defined by the gaging and sampling station at the Pumphouse location (38.922447, -
95 106.950828) near Mount Crested Butte, CO. The Pumphouse subcatchment has a large elevation gradient from 2700
96 to 4100 m (Figure 1) and is predominantly underlain by Paleozoic and Mesozoic sedimentary rocks, including Mancos
97 Shale that covers 44% of the catchment area, and localized intrusive igneous rocks like granodiorite (Gaskill et al.,
98 1991). The vegetation is dominated by shrubs, grasses, and forbs in the montane (<2800 m elevation, 2% of catchment
99 area), aspen and conifers in the lower subalpine (2800 to 3200 m, 34% of the catchment area) and conifers in the upper
100 subalpine (3200 to 3500 m, 32% of the catchment area) regions. In the alpine region (>3500 m, 31% of the catchment



101 area), shrubs are dominant until 3800 m, above which land is mostly barren (Carroll, Deems, Sprenger, et al., 2022).
102 Meadows are distributed across the catchment, but take up a relatively small share of the total area above the montane.
103 The climate is dominated by cold winters with substantial snow cover and snowpack accumulation that constitutes
104 about 80% of the total annual precipitation (Carroll, Deems, Sprenger, et al., 2022). Summers are relatively warm and
105 dry with monsoonal rain that accounts for 20% of the annual precipitation. The snowpack depth is generally greater
106 and snowmelt timing is later with increasing elevation across the catchment (Carroll et al., 2022a). The catchment
107 hydrograph is dominated by the snowmelt pulse with an onset in April, a pronounced peak during June and a
108 subsequent snowmelt recession interspersed with smaller peaks driven by monsoon rainfall events. Between
109 September and March, the catchment streamflow is generally limited to base flow (Carroll et al., 2020). The East
110 River has been intensely instrumented and studied since 2015; more details are provided in Hubbard et al. (2018).

111 In addition to the East River, we also sampled the Upper Gunnison River near Gunnison, CO, about 50 km downstream
112 from Mount Crested Butte. This catchment is defined by the USGS streamgage #09114500 (38.54193567, -
113 106.9497661) and has a drainage area of 2,618 km². A third basin was included, which is defined by the USGS
114 streamgage # 09095500 (39.2391463 -108.2661946) of the main stem of the Colorado River near Cameo, CO. Its
115 drainage area is of 20,683 km² (USGS Water Data for the Nation, 2023). Hereafter, these two basins locations are
116 referred to as Gunnison and Cameo, respectively, and their catchment areas are shown in Figure 1.

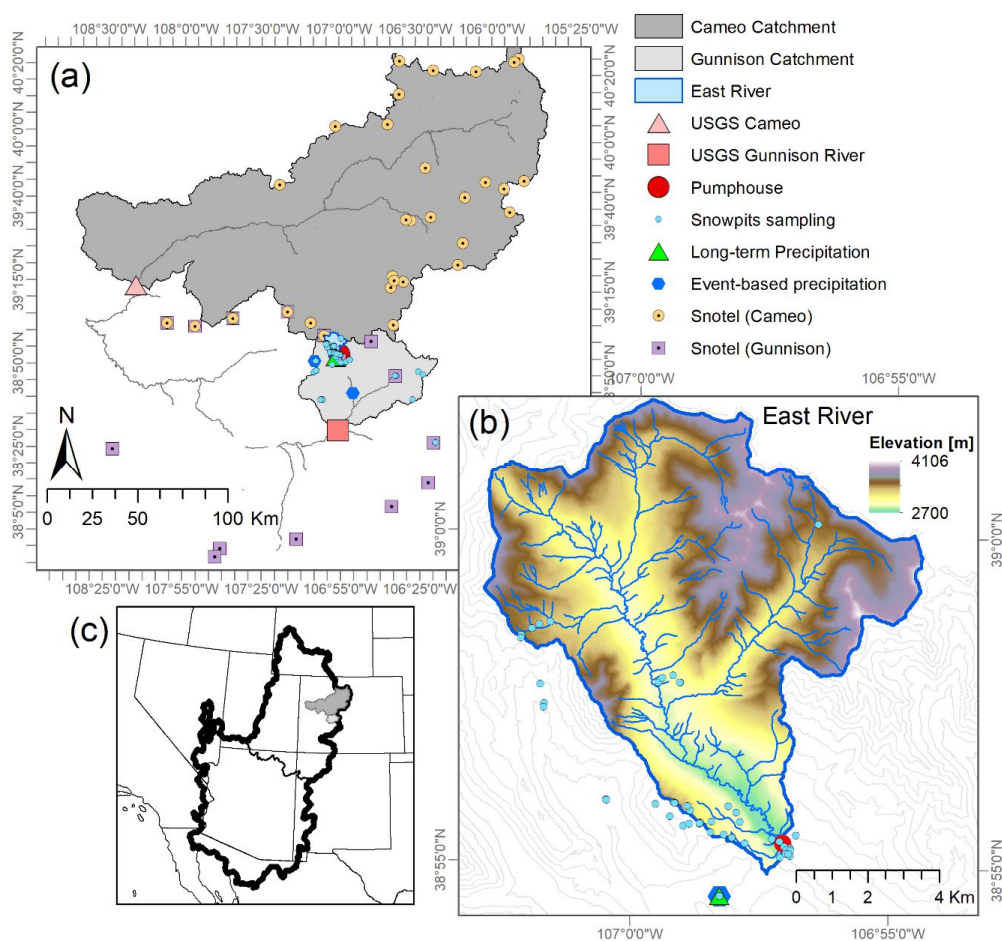
117 Within the Gunnison River Basin, there are 15 SNOTEL sites located at elevations ranging between 2674 and 3523
118 m providing snow water equivalent (SWE) observations (Suppl. Table 1). Across these SNOTEL sites, elevation was
119 not a good predictor for the maximum snowpack depth (Suppl. Fig. 1). For the Colorado River at Cameo, we chose
120 the 31 SNOTEL sites in the Colorado Headwaters ranging between 2610 and 3452 m (Report Generator 2.0, 2023)
121 (Figure 1).

122 We sampled snowpack between 2016 and 2019 across a gradient spanning 1324 m in elevation (from 2347 to 3671
123 m) in the Gunnison catchment (Figure 1a&b). A total of 53 snow pits were dug in flat areas with samples collected in
124 duplicate at 10-cm depth increments to tabulate snow density, temperature, and stable isotope ratios. Bulk snowpack
125 isotopic content represents the SWE-weighted composite value across the entire snow column (Carroll et al., 2022b).
126 Precipitation was first sampled on an event basis via a collector from 2014 to 2017 in Mount Crested Butte at 2885
127 m, and the sampling procedure was outlined in Carroll et al. (2022b). Since 2020, we sampled the precipitation on an
128 approximate event basis at the locations Estess (2513 m), Mount Crested Butte (2885 m), and Irwin Barn (3181 m).
129 (Figure 1). We sampled stream water from the East River at the Pumphouse location from 2014 to 2022 on daily to
130 fortnightly frequency. There was a gap of sampling in April 2018; and therefore, 2018 was excluded from the present
131 analyses. Sampling at the Gunnison River was done between March 2020 and December 2021 on a weekly basis with
132 occasional higher (3 days) or lower (15 days) frequency. At Cameo, stream water sampling occurred at weekly to
133 fortnightly frequency in 2021 and 2022.



134 All water samples were measured for stable hydrogen and oxygen isotopes using a Cavity Ring-Down Spectroscopy
135 (Picarro L2130-i). We report isotope ratios as $\delta^{18}\text{O}$ and $\delta^2\text{H}$ values expressed relative to the Vienna Standard Mean
136 Ocean Water.

137



138

139 **Figure 1** (a) Locations of streamgages and water sampling of the Colorado River near Cameo and the Gunnison River in
140 Gunnison (black markers) and the river's catchment area (grey). Locations of event-based precipitation sampling (blue
141 markers), SNOTEL stations in the Colorado (light blue) and Gunnison (light purple) areas. East River catchment area
142 (blue outline) as defined by Pumphouse gaging and sampling location (red circle) located within the Gunnison river
143 catchment also shown. (b) Area and elevation of the East River catchment with the streamgaging and water sampling location
144 at Pumphouse (red marker) and long-term precipitation sampling site (cyan triangle). (c) Locations of the catchments
145 defined by the stream gages near Cameo and Gunnison (light grey) in the Colorado River Basin (thick black line).

146 2.2 Data analyses

147 We calculated the deuterium excess value (short “*d-excess*”) for all water samples as defined by equation (2).



148 While it was shown that the *d-excess* of precipitation is on average about 11.27 ‰ on a global scale (Rozanski et al.,
149 1993), for snowpacks, the *d-excess* values were found to increase with elevation (Froehlich et al., 2008; Tappa et al.,
150 2016) due to increased evaporative fractionation from lower elevation snowpacks which are re-condensed at higher
151 elevations (Lambán et al., 2015). Because the slope of the local meteorologic water line, observed to be 7.4 (Carroll
152 et al., 2022b) near Mt Crested Butte and 7.2 at the lower elevation Gunnison site (Marchetti and Marchetti, 2019),
153 does not deviate much from the slope of 8 of the global meteorologic water line that defines the *d-excess* (see Suppl.
154 Fig. 2), we decided to use the *d-excess* rather than lc-excess (Landwehr and Coplen, 2006). We used linear correlation
155 analyses to describe various relation and provide Pearson (r) coefficients. For significant correlations ($p < 0.05$), we
156 added linear regression lines to the plots.

157 We used the SNOTEL data to compute the fraction of peak SWE through time for each water year (a value of one
158 equals maximum SWE and zero indicates the snowpack is melted). Because SNOTEL SWE data only reflects
159 conditions at the stations, we used spatially explicit snowmelt simulations, as published by Carroll et al. (2022a), that
160 were informed by the airborne snow observatory (ASO). For each water year with snowmelt simulations available,
161 we calculated the cumulative difference through time between the simulated snowmelt for the montane and alpine
162 elevation bands in the East River, given as millimeter (mm) SWE. In this case, a value of zero indicated equal
163 snowmelt volumes from the montane and alpine snowpack, whereas positive values show that alpine snowmelt
164 exceeded montane snowmelt.

165 We applied for each day with a stream water sample the Bayesian mixing framework HydroMix by Beria et al. (2020)
166 to estimate the temporal dynamics of the share of high elevation snowmelt in the streamflow during the snowmelt
167 period, which occurred between day 200 to 300 of the water year (water year starts on October 1st). The two end
168 members were defined as the *d-excess* of the snowpack from the upper subalpine and alpine snowpack (>3200 m,
169 $n=31$, defined as “high elevation”) and lower subalpine and montane area (<3200 m, $n=60$), respectively. We report
170 the mean fraction of high elevation snowmelt in each water sample with standard deviations based on the distribution
171 of the two endmembers as described in Beria et al. (2020). We further report the seasonal average and maximum share
172 of high elevation snowpack in the stream samples. We compared the HydroMix results with MixSIAR (Stock et al.,
173 2018) calculations and found with both methods very similar results. A multiple linear regression was used to explore
174 the predictability of the maximum share of high elevation snowmelt during the different years as a function of the
175 maximum SWE and the mean air temperature measured at the Gunnison SNOTEL sites during the snowmelt period.

176 **3 Results**

177 **3.1 The *d-excess* of stream water increased with high elevation snowmelt contributions**

178 Our snowpack sampling campaigns along a 1324 m elevation gradient showed that the average (\pm SD) *d-excess* value
179 of the high elevation (>3200 m) snowpack was 13.8 (± 1.6) ‰ and thus significantly higher than for the lower elevation
180 snowpack 10.7 (± 1.8) ‰ (Suppl. Fig. 3). The *d-excess* of the lower elevation snowpack was not significantly different
181 from groundwater (10.5 \pm 1.0 ‰, Suppl. Fig. 3) nor from the *d-excess* of summer rainfall (Suppl. Fig. 4). We further
182 observed a strong and temporally consistent (generally $r > 0.63$ and $p < 0.05$ for the four individual years) increase in



183 *d-excess* of the snowpack with elevation (Figure 2b). The *d-excess* lapse rate of the snowpack +0.52 ‰/100 m, leading
184 to 12.9 ‰ to 14.4 ‰ and 14.4 ‰ to 17.6 ‰ for the *d-excess* of the snowpack in the upper subalpine and alpine region,
185 respectively. Lapse rates for the snowpack were not seen in $\delta^{18}\text{O}$ (Figure 2b) or $\delta^2\text{H}$ (data not shown). The precipitation
186 sampled via collectors across the 667 m elevation gradient from the event-based sampler also showed a relation
187 between average *d-excess* and elevation for the samples collected weekly to fortnightly between November and April
188 during water years 2021 and 2022 (Suppl. Fig. 5). These samples reflect a *d-excess* lapse rate for winter precipitation
189 of +0.7 ‰/100 m, which was slightly higher than snowpack, though the elevation range for the precipitation sampler
190 was lower. There was generally a large variability of SWE dynamics across the SNOTEL sites in the Gunnison
191 catchment (Figure 3a), and this variation among the sites did not result from elevation differences (Suppl. Fig. 1).

192 The hydrograph of the snowmelt period had peak streamflow during May and June, a recession towards August and
193 lowest flows between September and March (Figure 3a). This pattern was consistent during the seven water years, but
194 years with lower SWE resulted in lower peak flows, as expected (Suppl. Fig. 6).

195 The stream water $\delta^{18}\text{O}$ dynamics reflected the seasonality of precipitation inputs, from having lower values (depleted
196 in ^{18}O) during peak flow and trending towards higher values (enriched in ^{18}O) during summer and early fall due to
197 greater fractional contributions from base flow and rainfall contributions that had higher $\delta^{18}\text{O}$ values compared to the
198 snowfall. Due to the strong difference in $\delta^{18}\text{O}$ values of rain and snowfall (see discussion in Sprenger et al., 2022), the
199 $\delta^{18}\text{O}$ of stream water decreased during the low flows in winter due to a higher fraction of groundwater sourced from
200 snowmelt vs. rain in the catchment runoff (orange points and line in Figure 3b). The $\delta^{18}\text{O}$ of snowmelt stream water
201 reached a minimum in June during maximum snowmelt contribution, after which the snowpack ceased to exist and
202 $\delta^{18}\text{O}$ of stream water increased throughout the summer with recession to base flow and monsoonal rainfall.

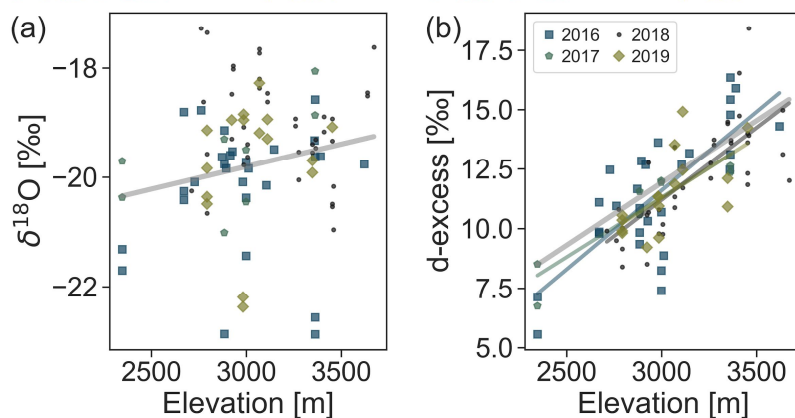
203 The *d-excess* values of stream water did not show a strong seasonal dynamic, but in general, *d-excess* values mainly
204 increased during the snowmelt season and subsequently dropped again during the summer (red points and line in
205 Figure 3b). The increase of *d-excess* of stream water was not due to the rainfall input because there was no seasonal
206 trend in *d-excess* of rainfall (Suppl. Fig. 4). Instead, *d-excess* of stream water resulted from melting snowpack at higher
207 elevations due to snowmelt progression, as evidenced by the SNOTEL SWE data, that resulted in increases in *d-excess*
208 of stream water consistently for each of the investigated years (Figure 4a). The hypothesis that this increase in *d-*
209 *excess* of stream water resulted from high elevation snowmelt contributions is supported by its relation with simulated
210 snowmelt differences between alpine and montane snowmelt volumes through time (Figure 4b). When the high
211 elevation snowmelt volumes became increasingly larger than the low elevation snowmelt, *d-excess* of stream water
212 increased consistently. Notably, Figure 4b also shows that stream water *d-excess* values of stream water were highest
213 for years with largest differences between alpine and montane snowpack (2017 and 2019).

214 Our *d-excess*-based endmember mixing analyses revealed that 41 to 57% of the flow in the East River during the
215 snowmelt period stemmed from high elevation snowpack (Figure 5 left). Periods when there were an increase in the
216 fraction of high elevation snowmelt contributions tend to be later in the snowmelt hydrograph and coincided with
217 periods of runoff intensification (Figure 5, right). During peak alpine snowmelt contributions, about two-third of the
218 East River flow stemmed from the high elevation snowpack. There was a general trend that the maximum high



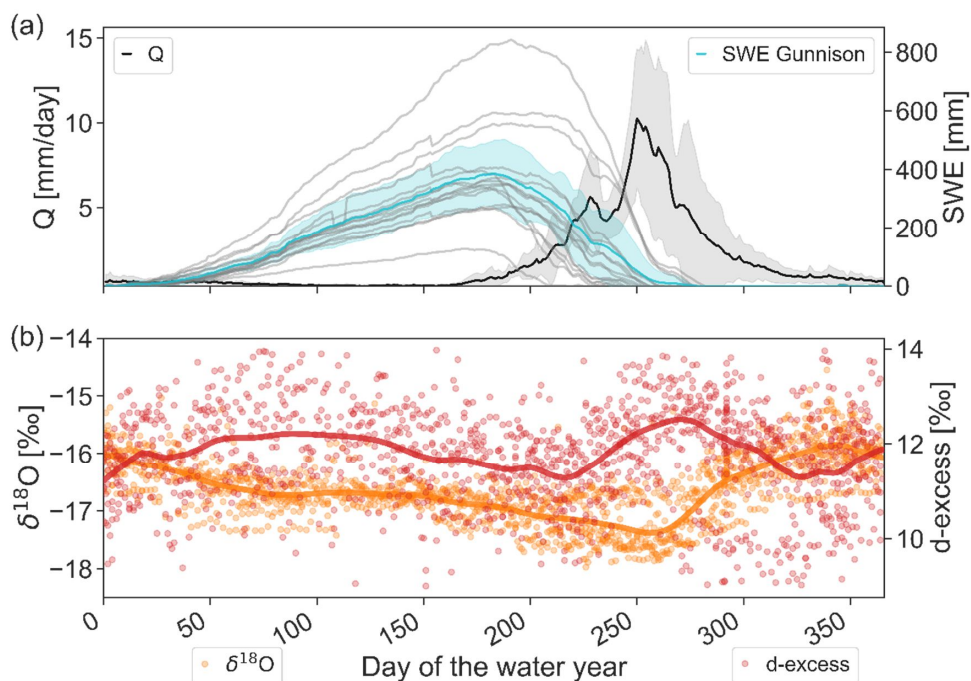
219 elevation snowpack contributions were higher in water years with lower SWE (Suppl. Fig. 7a, $r=-0.51$, $p=0.24$).
 220 However, the relatively warm snowmelt period of 2017, following a winter with deep snowpack, resulted in relatively
 221 large high elevation snowmelt contributions and thus did not follow that trend. Because of this observation, we
 222 included the average air temperature measured at the SNOTEL sites during the snowmelt period as a second variable
 223 in a multiple regression analysis. This regression explained 66% of the interannual variation of the maximum high
 224 elevation snowmelt contribution, and all variables had significance levels of <0.1 . Our results therefore indicate that
 225 the snowpack at the highest elevation can be more important for runoff generation in low-snow years and when the
 226 air temperature is higher (Figure 6). We also tested the streamflow volumes during the snowmelt period as a variable,
 227 but did not include it, because of its strong correlation with SWE_{max} ($r=0.84$, $p=0.018$).
 228

2016	2017	2018	2019	All years	2016	2017	2018	2019	All years
$r=0.08$	$r=0.57$	$r=-0.19$	$r=0.20$	$r=0.20$	$r=0.76$	$r=0.93$	$r=0.75$	$r=0.63$	$r=0.65$
$p=0.68$	$p=0.14$	$p=0.24$	$p=0.47$	$p=0.03$	$p=0.00$	$p=0.00$	$p=0.00$	$p=0.01$	$p=0.00$
$b=0.0003$	$b=0.0014$	$b=-0.0007$	$b=0.0011$	$b=0.0008$	$b=0.0066$	$b=0.0050$	$b=0.0061$	$b=0.0051$	$b=0.0052$
$a=-21.09$	$a=-23.71$	$a=-16.93$	$a=-23.04$	$a=-22.28$	$a=-8.25$	$a=-3.67$	$a=-7.01$	$a=-3.98$	$a=-3.78$



229
 230 **Figure 2** The $\delta^{18}O$ of snowpack (a) and d -excess (b) values sampled in the Upper Colorado River Basin during four different
 231 winters along an elevation gradient. Regression lines are plotted for correlations with $p<0.05$. For each year and for the
 232 bulk isotope data, Pearson correlation coefficients (r), significant levels (p), as well as slope (b), and intercept (a) of the
 233 regression are given.

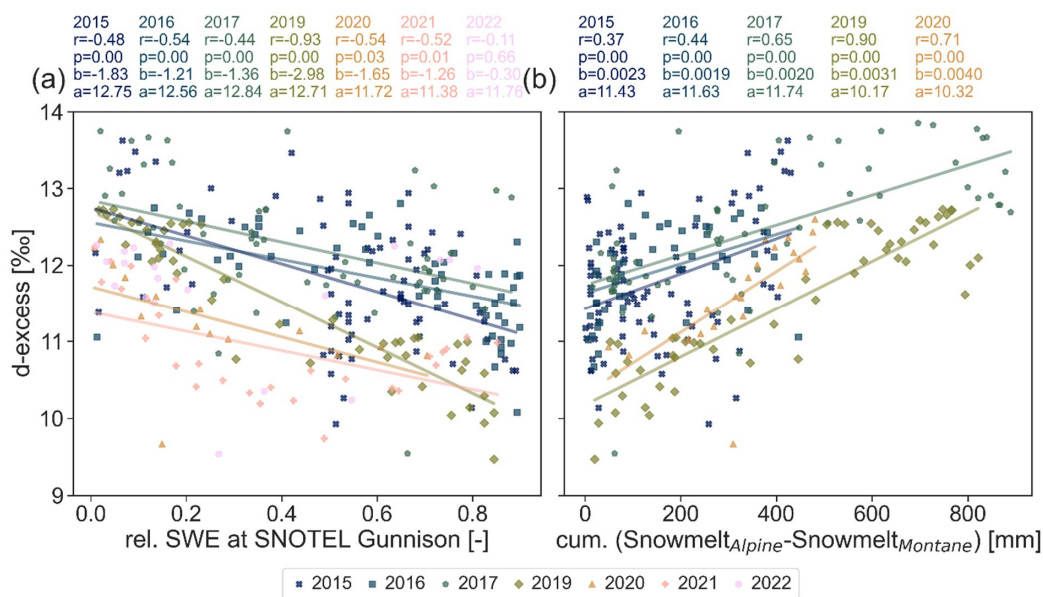
234



235

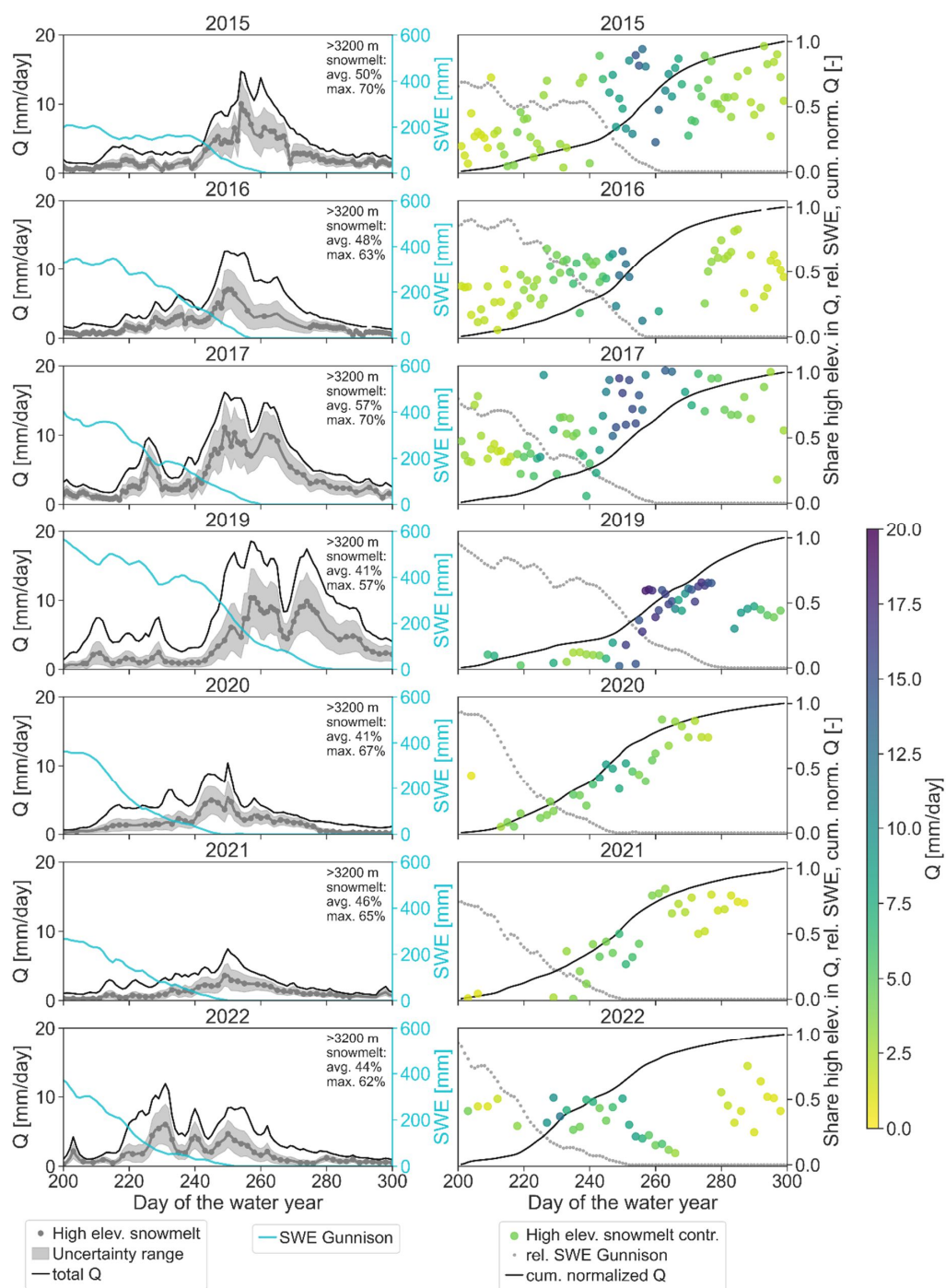
236 **Figure 3 (a) Median annual dynamics of East River streamflow (Q, black) and snow water equivalent (SWE) at the**
237 **individual SNOTEL sites within the Gunnison River catchment (grey) and the average of all sites (cyan) from water year**
238 **2015 to 2022 with semitransparent grey and cyan area representing the standard deviation of Q and SWE, respectively. (b)**
239 **The $\delta^{18}\text{O}$ (orange) and *d-excess* (red) of all stream water samples collected between water year 2015 and 2022 from the East**
240 **River at the Pumphouse location. The orange and red lines are a LOWESS fit to the data points. See Suppl. Fig. 6 for a**
241 **time series plot of the same data.**

242



243

244 **Figure 4 (a)** The *d-excess* of stream water values during snowmelt for seven individual years, shown as a function of relative
 245 snow water equivalent (SWE) measured at the SNOTEL stations across the Gunnison River catchment at the time of
 246 sampling. For each year, the Pearson correlation (r) and the associated significance level (p) are given as well as the intercept
 247 (a) and slope (b) of the regression. (b) The *d-excess* of stream water as a function of the cumulative differences between the
 248 simulated snowmelt at alpine (=highest elevation in the East River) and montane (lowest elevation in the East River) region
 249 at the time of each stream water collection. Regression lines are shown for $p \leq 0.05$.

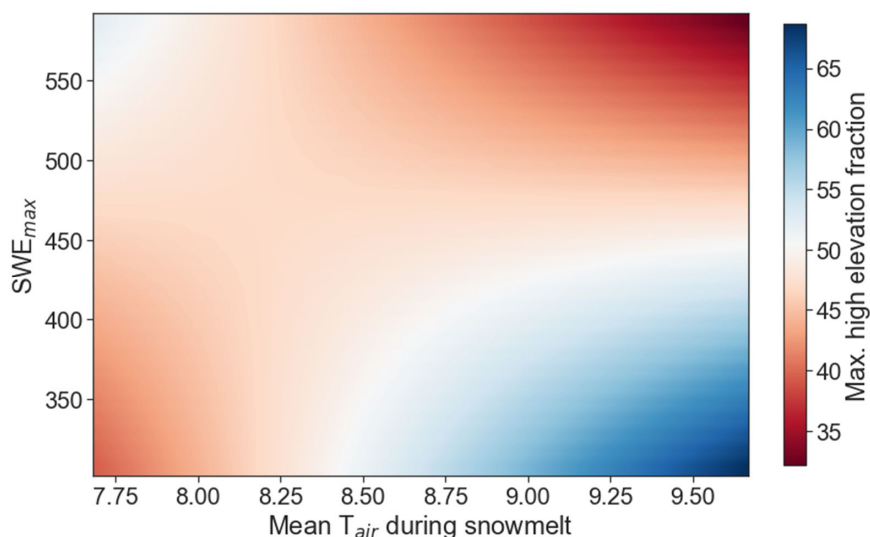


250

251 **Figure 5 (left) Endmember mixing analyses based on *d*-excess of stream water inferring the share of high elevation snowmelt**
 252 **(grey dots and lines) in the streamflow during the snowmelt-induced peak flow of the East River. The uncertainty range is**



253 shown as grey bands and it represents the standard deviation (22% on average). Additionally, we show the total streamflow
254 (Q , black line) as well as the snow water equivalent (SWE, cyan) for the SNOTEL sites in the Gunnison catchment. (right)
255 Share of high elevation snowmelt in the streamflow (points, color coded by Q), relative SWE in Gunnison ($1 = \text{peak SWE}$),
256 and cumulative streamflow between day 200 and 300 of the water year. Note that the y-axis for the graphs on the right is
257 plotted on the right-hand side.



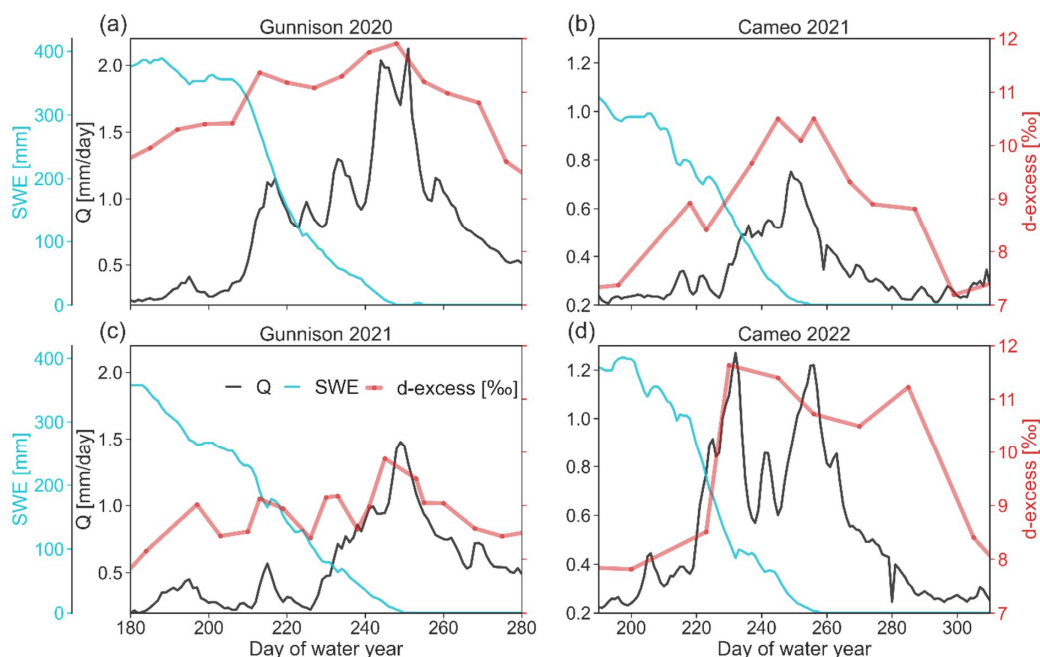
258

259 **Figure 6** Result of the multiple regression analyses to assess predictability of the maximum contribution of high elevation
260 snowmelt to stream water as a function of the maximum snow water equivalent (SWE_{max}) and the air temperature (T_{air})
261 during the snowmelt period measured at the SNOTEL sites in Gunnison. Note that the regression includes interaction
262 between SWE_{max} and T_{air} as follows: $-37.03 * T_{\text{air}} - 0.73 * SWE_{\text{max}} + 0.089 * T_{\text{air}} * SWE_{\text{max}} + 350.74$

263 3.2 The *d-excess* dynamics of stream water beyond headwaters

264 Downstream from the East River, the Gunnison River stream water samples showed similar increase in *d-excess* as
265 streamflow during the snowmelt season increased. This pattern was observed for both years in which stream water
266 sampling in Gunnison was done. In 2020, the snowpack was deeper, and the runoff was higher than in 2021.
267 Additionally, the *d-excess* values of stream water were different for the different years with generally higher values
268 for 2020 than in 2021 (Figure 7a,c). Despite 30 times larger drainage area of the Gunnison River compared to the East
269 River, the effect of the high elevation snowmelt on the *d-excess* measurements of stream water was detectable, albeit
270 dampened given the greater fraction of lower elevations contributing to its flow.

271 The drainage area of the Colorado River near Cameo is eight times the drainage area of the Gunnison River, but the
272 difference between the *d-excess* of stream water at the beginning and end of the snowmelt period was greater than 3
273 % in 2021 and 2022. Thus, despite the large catchment area of the Colorado River near Cameo, and greater mixing
274 of runoff in reservoirs within that catchment, the snowmelt contribution from high elevation regions was substantial
275 during the snowmelt peak flow (Figure 7b,d).



276

277 **Figure 7** Streamflow (Q, black) and *d-excess* (red dots and line) of the stream water before and during snowmelt for the
278 Gunnison River near Gunnison, Colorado in 2020 (a) and 2021 (c) and for the Colorado River near Cameo, Colorado for
279 2021 (b) and 2022 (d). Further shown is the average snow water equivalent (SWE, cyan line) of all the SNOTEL sites located
280 in the Gunnison catchment and in the Colorado River eadwaters for the Cameo site, respectively. Note that the y-axes
281 have different scales for each subplot.

282

283 4 Discussion

284 4.1 The *d-excess* of stream water reflects high elevation snowmelt

285 We find that *d-excess* of stream water can be used to differentiate the effects of snowmelt from low vs. high elevations
286 using three independent approaches: First, the comparisons of *d-excess* dynamics of stream water with the observed
287 snowpack reduction at SNOTEL sites in the region showed a strong relation that was consistent during six of the seven
288 investigated snowmelt periods (Figure 4a). The SNOTEL data do not show an increased snowpack with elevation
289 (Suppl. Fig. 1), but ASO flight data indicate that snowpack depth generally increases with elevation (Carroll, Deems,
290 Sprenger, et al., 2022). Thus, with decreasing SWE during the snowmelt period, the ratio of high elevation snowmelt
291 can increase. Such a trend of relative increase of the high elevation snowpack during low snow years was observed.
292 Second, simulated differences based on spatially explicit hydrological modeling of snowmelt timing and volumes
293 between the montane and alpine regions within the East River catchment correlated significantly with *d-excess* of
294 stream water for every simulated snowmelt period (Figure 4b). Third, the increase in *d-excess* of stream water
295 coincided with the peak streamflow during each snowmelt period (with exception for 2022, Figure 5). Thus, elevated
296 *d-excess* values cannot stem from low elevation snowmelt but most likely result from higher elevation snowmelt as



297 the snowmelt generally progresses from lower to higher elevations due to the temperature gradients across the
298 catchment.

299 Because we observed consistent lapse rates of *d-excess* values in the snowpack during several years (Figure 2b),
300 significant differences between the *d-excess* at lower and higher elevation snowpack (Suppl. Fig. 3), and also a *d-*
301 *excess* lapse rate in the winter precipitation (Suppl. Fig. 5), we see a great potential for *d-excess* measurements to serve
302 as a tracer for endmember-mixing analyses to derive high elevation snowmelt contributions to the catchment's
303 streamflow during snowmelt periods.

304 Other studies have also shown that snowpack at highest elevations had the highest *d-excess* values; data by Froehlich
305 et al. (2008) indicate a lapse rate for *d-excess* values of +0.2 ‰/100 m across an elevation range between 469 and
306 2245 m across the Alps, and data published by Tappa et al. (2016) indicate a lapse rate of +0.38 ‰/100 m in the Rocky
307 Mountains in Idaho. Our lapse rate of +0.52 ‰/100 m was slightly higher than those reported by others. However, the
308 sampling strategies for the different studies are different, and importantly, the general trend of increased *d-excess*
309 values with elevation was the same for all three studies in mountainous systems.

310 A potential explanation for how *d-excess* lapse rates in the snowpack develop is sublimation of snow at lower elevation
311 and the subsequent condensation of the water vapor at colder higher elevation (Beria et al., 2018; Lambán et al., 2015).
312 Our long-term sampling of the precipitation in the East River can further rule out a potential precipitation *d-excess*
313 seasonality to influence the *d-excess* of stream water during the snowmelt period (Suppl. Fig. 4). Therefore, there are
314 several independent data sources that all point towards high elevation snowmelt contributions to the catchment
315 streamflow driving the observed *d-excess* of stream water variation during the snowmelt period.

316 Our findings, based on endmember-mixing analyses via *d-excess* values highlight the importance of high elevation
317 snowpack for runoff generation. The interannual variation in *d-excess* of stream water and the derived high elevation
318 snowmelt contributions indicate that the snowpack of the upper subalpine and alpine region could be most important
319 in years of relatively low snowpack accumulation and comparably high spring air temperatures. Thus, with the
320 projection of a reduced snowpack in the western United States (Siirila-Woodburn et al., 2021), understanding the high
321 elevation snowpack dynamics could most likely become more important, and *d-excess* observations are a tool to
322 investigate the timing (e.g., trend towards earlier melt) and fate (e.g., streamflow contribution vs. sublimation or
323 groundwater recharge) of the snowpack throughout the melting period.

324 **4.2 Limitations and opportunities of *d-excess* of stream water with scale**

325 Our results show that the *d-excess* patterns of stream water observed in a headwater stream can be upscaled because
326 we see a similar *d-excess* pattern of stream water at larger scales from stream water sampling in Gunnison and Cameo.
327 The latter sampling site is an entirely different catchment to the north of East River and Gunnison River in which the
328 snowpack was not sampled for its *d-excess* values. However, the *d-excess* signal of stream water for Coal Creek, a
329 smaller headwater catchment to the west of the East River catchment, did not show a similar pattern (Suppl. Fig. 8,
330 Suppl. Fig. 9), likely because of a lower representation of high elevation bands within in the catchment (Suppl. Fig.
331 10). Twenty nine percent of the Coal Creek catchment area is the upper subalpine region, but only 6% of the catchment
332 is alpine (>3500 m). Thus, high elevation snowpack with the highest *d-excess* values is essentially missing in Coal
333 Creek, which presumably dampened *d-excess* response of stream water. We therefore hypothesize that the



334 applicability of the *d-excess* of stream water as a signal for high elevation snowmelt is dependent on a sufficient area
335 with high elevation (>3200 m) and sufficient elevation gradient in the catchment of the sampled stream. Lastly,
336 although we see *d-excess* dynamics of stream water in response to high elevation snowmelt at relatively large scales,
337 the isotope dynamics may likely not be detectable downstream from large reservoirs. Initial sampling of the Colorado
338 River near the Colorado-Utah state line with a drainage area of 46,230 km² that includes several large reservoirs
339 indicates that stream water *d-excess* changes are rather dampened and might not hold sufficient information to infer
340 high elevation snowmelt contributions (not shown).

341 Because snowpack volumes are getting lower, and snowmelt is starting earlier in mountainous regions due to climate
342 change (Musselman et al., 2021), we need to find ways to assess the effect of these both at sub-annual to decadal time
343 scales. Short term identification of a snow drought could allow for adaptive water management measures on the sub-
344 annual time scale, whereas long-term trends might show the trajectory of mountain snow dynamics. With 0.2 ‰
345 measurement uncertainty of the *d-excess* values due to 0.025 ‰ and 0.1 ‰ precision (1σ) in δ¹⁸O and δ²H,
346 respectively, the observed variation of *d-excess* in snowpack and stream water are at least ten times larger. Our results
347 and the discussion in the previous section show that measurements of *d-excess* of stream water is a relatively cost-
348 effective way to obtain catchment integrated information about the high elevation snowpack.

349 Although SNOTEL sites are point measurements and therefore do not represent integrated patterns across
350 heterogeneous mountainous regions, *d-excess* of stream water does integrate throughout catchment areas. The lidar
351 based ASO data provide spatially explicit snowpack observations on catchment scales, but such data collection is
352 costly and represents only snapshots in time, although time series changes of snowpack during the snowmelt period
353 might be more informative. The costs of large-scale flight-based data collection may also make monitoring of
354 interannual SWE changes difficult to conduct over every basin where trends induced by climate change need to be
355 identified. The *d-excess* application introduced in this study is cost effective, applicable across scales that vary by
356 orders of magnitude, and needs limited labor and instrumental investments for the water sampling (e.g., autosampler)
357 and standardized laboratory analyses (e.g., laser spectrometer).

358 We suggest that *d-excess* of stream water could serve as a complementary information source in addition to the
359 currently applied streamflow shape and flashiness at low and high flows to derive relations between snow persistence
360 effects on the hydrograph across different climates (Le et al., 2022).

361 Measurements of *d-excess* of stream water can further help disentangling rapid high elevation snowmelt contributions
362 to the streamflow versus groundwater inflow to the stream. This is important because mountainous catchments with
363 lower groundwater influence were found to be more sensitive to snowpack changes due to warming (Tague and Grant,
364 2009).

365 **5 Conclusion**

366 Our snowpack and stream water stable hydrogen and oxygen isotope sampling program during several years links *d-*
367 *excess* of stream water at the catchment outlet to high elevation snowmelt contributions during the snowmelt period.
368 The relation between *d-excess* of stream water and snowmelt dynamics at high elevations was consistent during several
369 years. End member mixing analyses based on *d-excess* values quantified the temporal dynamics of high elevation
370 snowmelt contributions and its importance for the runoff generation from mountainous catchments. As compared to



371 other approaches, such catchment integrated information is a cost-effective way to better quantify the role of upper
372 subalpine and alpine snowpack for streamflow contributions in snow-dominated mountainous systems. Our findings
373 indicate that high elevation snowpack contributions to the streamflow tend to be more important during years with
374 lower snowpack and warmer spring temperatures. Thus, the high elevation snowpack could likely play a bigger role
375 in the coming decades as snowpack reduces and air temperature rise.

376 We hypothesize that transferability of this approach could depend on the share of high elevation regions of the
377 catchment area to contribute to streamflow, the presence of a *d-excess* lapse rate in the snowpack, and the absence of
378 large reservoirs upstream from the isotope sampling location. With increasing availability of stable isotope data of
379 mountainous catchments across the globe, future synthesis work could investigate the role of high elevation snowmelt
380 contributions in headwater regions worldwide.

381 **Data availability**

382 The data on East River streamflow (Newcomer et al., 2022), snowpack (Carroll et al., 2021) precipitation and stable
383 isotopes of stream water (Williams et al., 2020) are available online as cited. Snow water equivalent data from the
384 SNOTEL sites are available at <https://wcc.sc.egov.usda.gov/reportGenerator/>, streamflow and water stable hydrogen
385 and oxygen isotope data from the Gunnison and Cameo sites are available from USGS National Water Information
386 System (NWIS; <https://doi.org/10.5066/F7P55KJN>) database.

387 **Code availability**

388 The HydroMix code by Beria et al. (2019) is available on GitHub at
389 https://github.com/harshberia93/HydroMix/tree/20191007_GMD (last access: 20 August 2023).

390 **Acknowledgements**

391 This work was supported by the US Department of Energy Office of Science under contract DE-AC02-05CH11231
392 as part of Lawrence Berkeley National Laboratory Watershed Function Science Focus Area. We would like to express
393 appreciation to the Rocky Mountain Biological Laboratory for handling Forest Service permitting. We thank Jarral
394 Ryter in the WCU Chemistry program for analytical help with Cavity Ring-Down Spectroscopy. Any use of trade,
395 firm, or product names is for descriptive purposes only and does not imply endorsement by the U.S. Government.

396 **Author contributions**

397 MS conducted the data analysis and wrote the initial draft of the manuscript. All co-authors contributed either to the
398 analyses, the database, and the interpretation of both as well as improving the manuscript.

399 **Competing interests**

400 The authors declare that they have no conflict of interest.

401 **Competing interests**



402 The authors declare no competing interests.

403 **References**

404 Bennett, K. E. and Talsma, C.: Concurrent Changes in Extreme Hydroclimate Events in the Colorado River Basin,
405 *Water*, 13, 978, <https://doi.org/10.3390/w13070978>, 2021.

406 Beria, H., Larsen, J. R., Ceperley, N. C., Michelon, A., Vennemann, T., and Schaeffli, B.: Understanding snow
407 hydrological processes through the lens of stable water isotopes, *Wiley Interdiscip. Rev. Water*, 5, e1311,
408 <https://doi.org/10.1002/wat2.1311>, 2018.

409 Beria, H., Larsen, J. R., Michelon, A., Ceperley, N. C., and Schaeffli, B.: HydroMix v1.0: a new Bayesian mixing
410 framework for attributing uncertain hydrological sources, *Geosci. Model Dev.*, 13, 2433–2450,
411 <https://doi.org/10.5194/gmd-13-2433-2020>, 2020.

412 Bureau of Reclamation: Colorado River Basin Water Supply and Demand Study Executive Summary, Reclam.
413 Manag. Water West, 2012.

414 Carroll, R. W. H., Deems, J. S., Niswonger, R., Schumer, R., and Williams, K. H.: The Importance of Interflow to
415 Groundwater Recharge in a Snowmelt-Dominated Headwater Basin, *Geophys. Res. Lett.*, 46, 5899–5908,
416 <https://doi.org/10.1029/2019GL082447>, 2019.

417 Carroll, R. W. H., Manning, A. H., Niswonger, R., Marchetti, D., and Williams, K. H.: Baseflow Age Distributions
418 and Depth of Active Groundwater Flow in a Snow-Dominated Mountain Headwater Basin, *Water Resour. Res.*, 56,
419 e2020WR028161, <https://doi.org/10.1029/2020WR028161>, 2020.

420 Carroll, R. W. H., Deems, J., Sprenger, M., Maxwell, R., Brown, W., Newman, A., Beutler, C., and Williams, K. H.:
421 Modeling Snow Dynamics and Stable Water Isotopes Across Mountain Landscapes, *Geophys. Res. Lett.*, 49,
422 e2022GL098780, <https://doi.org/10.1029/2022GL098780>, 2022a.

423 Carroll, R. W. H., Deems, J., Maxwell, R., Sprenger, M., Brown, W., Newman, A., Beutler, C., Bill, M., Hubbard, S.
424 S., and Williams, K. H.: Variability in observed stable water isotopes in snowpack across a mountainous watershed in
425 Colorado, *Hydrol. Process.*, 36, e14653, <https://doi.org/10.1002/hyp.14653>, 2022b.

426 Craig, H.: Isotopic variations in meteoric waters, *Science*, 133, 1702–1703,
427 <https://doi.org/10.1126/science.133.3465.1702>, 1961.

428 Dansgaard, W.: Stable isotopes in precipitation, *Tellus*, 16, 436–468, <https://doi.org/10.1111/j.2153-3490.1964.tb00181.x>, 1964.

430 Dozier, J., Bair, E. H., and Davis, R. E.: Estimating the spatial distribution of snow water equivalent in the world's
431 mountains, *WIREs Water*, 3, 461–474, <https://doi.org/10.1002/wat2.1140>, 2016.

432 Fassnacht, S. R., Dressler, K. A., and Bales, R. C.: Snow water equivalent interpolation for the Colorado River Basin
433 from snow telemetry (SNO^{TEL}) data, *Water Resour. Res.*, 39, <https://doi.org/10.1029/2002WR001512>, 2003.

434 Faybishenko, B., Arora, B., Dwivedi, D., and Brodie, E.: Statistical framework to assess long-term spatio-temporal
435 climate changes: East River mountainous watershed case study, *Stoch. Environ. Res. Risk Assess.*,
436 <https://doi.org/10.1007/s00477-022-02327-7>, 2022.

437 Freudiger, D., Kohn, I., Seibert, J., Stahl, K., and Weiler, M.: Snow redistribution for the hydrological modeling of
438 alpine catchments, *Wiley Interdiscip. Rev. Water*, 4, e1232, <https://doi.org/10.1002/wat2.1232>, 2017.



- 439 Froehlich, K., Kralik, M., Papesch, W., Rank, D., Scheifinger, H., and Stichler, W.: Deuterium excess in precipitation
440 of Alpine regions - Moisture recycling, *Isotopes Environ. Health Stud.*, 44, 61–70,
441 <https://doi.org/10.1080/10256010801887208>, 2008.
- 442 Gaskill, D. L., Mutschler, F. E., and Kramer, J. H.: Geologic map of the Gothic Quadrangle, Gunnison County,
443 Colorado, <https://doi.org/10.3133/gq1689>, 1991.
- 444 Gat, J. R.: Atmospheric water balance-the isotopic perspective, *Hydrol. Process.*, 14, 1357–1369,
445 [https://doi.org/10.1002/1099-1085\(20000615\)14:8<1357::AID-HYP986>3.0.CO;2-7](https://doi.org/10.1002/1099-1085(20000615)14:8<1357::AID-HYP986>3.0.CO;2-7), 2000.
- 446 Hammond, J. C., Sexstone, G. A., Putman, A. L., Barnhart, T. B., Rey, D. M., Driscoll, J. M., Liston, G. E., Rasmussen,
447 K. L., McGrath, D., Fassnacht, S. R., and Kampf, S. K.: High Resolution SnowModel Simulations Reveal Future
448 Elevation-Dependent Snow Loss and Earlier, Flashier Surface Water Input for the Upper Colorado River Basin, *Earths
449 Future*, 11, e2022EF003092, <https://doi.org/10.1029/2022EF003092>, 2023.
- 450 Hoerling, M., Barsugli, J., Livneh, B., Eischeid, J., Quan, X., and Badger, A.: Causes for the century-long decline in
451 Colorado river flow, *J. Clim.*, 32, 8181–8203, <https://doi.org/10.1175/JCLI-D-19-0207.1>, 2019.
- 452 Hubbard, S. S., Williams, K. H., Agarwal, D., Banfield, J., Beller, H., Bouskill, N., Brodie, E., Carroll, R., Dafflon,
453 B., Dwivedi, D., Falco, N., Faybishenko, B., Maxwell, R., Nico, P., Steefel, C., Steltzer, H., Tokunaga, T., Tran, P.
454 A., Wainwright, H., and Varadharajan, C.: The East River, Colorado, Watershed: A Mountainous Community Testbed
455 for Improving Predictive Understanding of Multiscale Hydrological–Biogeochemical Dynamics, *Vadose Zone J.*, 17,
456 180061, <https://doi.org/10.2136/vzj2018.03.0061>, 2018.
- 457 Immerzeel, W. W., Lutz, A. F., Andrade, M., Bahl, A., Biemans, H., Bolch, T., Hyde, S., Brumby, S., Davies, B. J.,
458 Elmore, A. C., Emmer, A., Feng, M., Fernández, A., Haritashya, U., Kargel, J. S., Koppes, M., Kraaijenbrink, P. D.
459 A., Kulkarni, A. V., Mayewski, P. A., Pacheco, P., Painter, T. H., Pellicciotti, F., Rajaram, H., Rupper, S., Sinisalo,
460 A., Shrestha, A. B., Viviroli, D., Wada, Y., Xiao, C., Yao, T., and Baillie, J. E. M.: Importance and vulnerability of
461 the world ' s water towers, *Nature*, 577, <https://doi.org/10.1038/s41586-019-1822-y>, 2020.
- 462 Kendall, C. and McDonnell, J. J.: *Isotope tracers in catchment hydrology*, Elsevier, Amsterdam, Netherlands, 839 pp.,
463 1998.
- 464 Lambán, L. J., Jódar, J., Custodio, E., Soler, A., Sapriza, G., and Soto, R.: Isotopic and hydrogeochemical
465 characterization of high-altitude karst aquifers in complex geological settings. The Ordesa and Monte Perdido
466 National Park (Northern Spain) case study, *Sci. Total Environ.*, 506–507, 466–479,
467 <https://doi.org/10.1016/j.scitotenv.2014.11.030>, 2015.
- 468 Landwehr, J. M. and Coplen, T. B.: Line-conditioned excess: a new method for characterizing stable hydrogen and
469 oxygen isotope ratios in hydrologic systems, *Int. Conf. Isot. Environ. Stud.*, 132–135, 2006.
- 470 Le, E., Ameli, A., Janssen, J., and Hammond, J.: Snow Persistence Explains Stream High Flow and Low Flow
471 Signatures with Differing Relationships by Aridity and Climatic Seasonality, *Hydrol. Earth Syst. Sci. Discuss.*, 1–22,
472 <https://doi.org/10.5194/hess-2022-106>, 2022.
- 473 Marchetti, D. W. and Marchetti, S. B.: Stable isotope compositions of precipitation from Gunnison, Colorado 2007–
474 2016: implications for the climatology of a high-elevation valley, *Heliyon*, 5, e02120,
475 <https://doi.org/10.1016/j.heliyon.2019.e02120>, 2019.
- 476 Musselman, K. N., Addor, N., Vano, J. A., and Molotch, N. P.: Winter melt trends portend widespread declines in
477 snow water resources, *Nat. Clim. Change*, 11, 418–424, <https://doi.org/10.1038/s41558-021-01014-9>, 2021.
- 478 Report Generator 2.0: <https://wcc.sc.egov.usda.gov/reportGenerator/>, last access: 31 January 2023.



- 479 Painter, T. H., Berisford, D. F., Boardman, J. W., Bormann, K. J., Deems, J. S., Gehrke, F., Hedrick, A., Joyce, M.,
480 Laidlaw, R., Marks, D., Mattmann, C., McGurk, B., Ramirez, P., Richardson, M., Skiles, S. M. K., Seidel, F. C., and
481 Winstral, A.: The Airborne Snow Observatory: Fusion of scanning lidar, imaging spectrometer, and physically-based
482 modeling for mapping snow water equivalent and snow albedo, *Remote Sens. Environ.*, 184, 139–152,
483 <https://doi.org/10.1016/j.rse.2016.06.018>, 2016.
- 484 Rozanski, K., Araguás-Araguás, L., and Gonfiantini, R.: Isotopic patterns in modern global precipitation, in: *Climate*
485 *Change in Continental Isotopic Records*, vol. 78, edited by: Swart, P. K., Lohmann, K. C., McKenzie, J., and Savin,
486 S., American Geophysical Union, Washington, D. C., 1–36, <https://doi.org/10.1029/GM078p0001>, 1993.
- 487 Schneider, D. and Molotch, N. P.: Real-time estimation of snow water equivalent in the Upper Colorado River Basin
488 using MODIS-based SWE Reconstructions and SNO^{TEL} data, *Water Resour. Res.*, 52, 7892–7910,
489 <https://doi.org/10.1002/2016WR019067>, 2016.
- 490 Siirila-Woodburn, E. R., Rhoades, A. M., Szinai, J., Tague, C., Nico, P. S., and Huning, L. S.: A low-to-no snow
491 future and its impacts on water resources in the western United States, *Nat. Rev. Earth Environ.*, 2, 800–819,
492 <https://doi.org/10.1038/s43017-021-00219-y>, 2021.
- 493 Sprenger, M., Carroll, R. W. H., Dennedy-frank, J., Siirila-woodburn, E. R., Newcomer, M. E., Brown, W., and
494 Williams, K. H.: Variability of Snow and Rainfall Partitioning Into Evapotranspiration and Summer Runoff Across
495 Nine Mountainous Catchments, *Geophys. Res. Lett.*, 49, e2022GL099324, <https://doi.org/10.1029/2022GL099324>,
496 2022.
- 497 Stock, B. C., Jackson, A. L., Ward, E. J., Parnell, A. C., Phillips, D. L., and Semmens, B. X.: Analyzing mixing
498 systems using a new generation of Bayesian tracer mixing models, *PeerJ*, 6, e5096, <https://doi.org/10.7717/peerj.5096>,
499 2018.
- 500 Tague, C. and Grant, G. E.: Groundwater dynamics mediate low-flow response to global warming in snow-dominated
501 alpine regions, *Water Resour. Res.*, 45, <https://doi.org/10.1029/2008WR007179>, 2009.
- 502 Tappa, D. J., Kohn, M. J., McNamara, J. P., Benner, S. G., and Flores, A. N.: Isotopic composition of precipitation in
503 a topographically steep, seasonally snow-dominated watershed and implications of variations from the Global
504 Meteoric Water Line, *Hydrol. Process.*, 30, 4582–4592, <https://doi.org/10.1002/hyp.10940>, 2016.
- 505 USGS Water Data for the Nation: <https://dashboard.waterdata.usgs.gov/>, last access: 31 January 2023.
- 506
- 507